Applied Geochemistry 190 (2025) 106465

Contents lists available at ScienceDirect

Applied Geochemistry

journal homepage: www.elsevier.com/locate/apgeochem

Complexation of Cm(III) with monosilicic acid in chloride media

Sema Özyagan [a,*], Kim J. Warth [a], Thomas Sittel [b], Petra J. Panak [a,b]

[a] *Heidelberg University, Institut für Physikalische Chemie, Im Neuenheimer Feld 253, 69120, Heidelberg, Germany*
[b] *Karlsruhe Institute of Technology (KIT), Institute for Nuclear Waste Disposal (INE), P.O. Box 3640, 76021, Karlsruhe, Germany*

ARTICLE INFO

Editorial handling by: Dr Dmitrii A. Kulik

Keywords:
Curium(III)
Monosilicic acid
Complexation
Stability constant
Thermodynamic data

ABSTRACT

In this work, we present a detailed complexation study of Cm(III) with monosilicic acid in a NaCl medium at low to medium ionic strengths ($I_m = 0.01$–3.00 m). The complexation has been monitored using time-resolved laser fluorescence spectroscopy (TRLFS) in the pH_m range of 4–6. The results show that the formation of the monosilicate complex, $[\mathrm{Cm(H_3SiO_4)}]^{2+}$, is decreased with increasing ionic strength, leading to vast changes in the complex stability constant. Using the Specific Ion Interaction Theory (SIT), we were able to determine the complex stability constant at ionic strength $I_m = 0$ with $\log K_m^0 = 8.1 \pm 0.8$ and the binary ion-ion interaction coefficient $\varepsilon\ ([\mathrm{Cm(H_3SiO_4)}]^{2+}, \mathrm{Cl}^-) = 0.40 \pm 0.04$. Additionally, we studied the complexation at elevated temperatures at low to medium ionic strength. Using the van't Hoff equation, $\Delta_r H_m^0 = 16.4 \pm 0.5\ \mathrm{kJ\ mol^{-1}}$, $\Delta_r S_m^0 = 210 \pm 21\ \mathrm{J\ K^{-1}\ mol^{-1}}$ and the free Gibbs Energy $\Delta_r G_m^0 = -46.2 \pm 5\ \mathrm{kJ\ mol^{-1}}$ have been determined. These results show that the complexation reaction is endothermic and driven by an increase of entropy. These novel results obtained in a wide range of various ionic strengths are very important for the modeling of actinide behavior under near-field conditions of a nuclear waste repository in clay formations containing pore and formation waters with increased ionic strength.

1. Introduction

Cementitious materials are used for conditioning of different nuclear waste types and as components of waste containers or structural materials at the interface of backfilling and host-rock. As part of the multi-barrier system, they contribute to the retention of radionuclides. In case of water intrusion into the repository, cement degradation processes may occur. In such a scenario, released Si species can reach concentrations of up to 10^{-3} M. The chemistry of monomeric and polymeric silicates in aqueous solutions is quite versatile. The silicate speciation highly depends on various factors such as the total Si concentration, pH, ionic strength and temperature.

H_4SiO_4 is a weak acid ($-\log K_a = 9.82$) (Titulaer et al., 1994) and tends to condense and polymerizes into dimeric, trimeric, tetrameric, and oligomeric structures ($\mathrm{Si_2O_3(OH)_4^{2-}}$, $\mathrm{Si_3O_5(OH)_5^{3-}}$, $\mathrm{Si_4O_8(OH)_4^{4-}}$) with rising pH_m through the elimination of water (Dietzel, 2000). At low pH_m values, mainly the monosilicic acid $\mathrm{H_3SiO_4^-}$ is present, while polymerization occurs at pH_m values from 5 to 8 (Lagerström, 1959). Besides the pH_m value, the ionic strength also has an influence on polymerization. Metal cations such as $\mathrm{Na^+}$ reduce the electrostatic repulsion between the silicate anions, resulting in increased polymer formation (Choppin et al., 2008)’(Coradin et al., 2004)’ (Ray and Plaisted, 1983).

Actinides show strong interactions with silicates in aqueous systems (Kim et al., 2003), (Kim et al., 2008). In regards to the safety of nuclear waste disposal, complexation studies of uranium and transuranium elements (Np, Pu, Am, Cm) with silicates are of high importance. Literature studies focused on the complexation of U(VI) ion (Porter and Weber, 1971)’ (Satoh and Choppin, 1992)’ (Moll et al., 1998), Eu(III) (Jensenf and Choppin, 1996) and Am(III) (Wadsak et al., 2000) with monosilicate at low ionic strength. Most of these studies were performed in perchlorate media at silicate concentrations at around $[\mathrm{Si}] = 10^{-3} - 10^{-2}\ \mathrm{mol\ kg^{-1}}$ within a pH_m range of $pH_m = 3-6$. These conditions were carefully selected to ensure the presence of monosilicate in the system. At higher silicate concentrations and higher pH_m values, the silicate speciation is mainly influenced by polymeric silicate species, making analysis of the complexation of An(III) with monosilicate difficult.

In Pathak et al., the ionic strength was varied from $I_m(\mathrm{NaClO_4}) = 0.20$–$1.0\ \mathrm{mol\ kg^{-1}}$. From these results, the stability constant at zero ionic strength was determined $\left(\log K_m^0\left([\mathrm{CmH_3SiO_4}]^{2+}\right) = 8.60 \pm 0.08\right)$ using the SIT (Pathak and Choppin, 2006). In chloride media, Panak et al. determined $\log K_m\left([\mathrm{CmH_3SiO_4}]^{2+}\right) = 7.32 \pm 0.08$ (Panak et al.,

---

* Corresponding author.
E-mail address: sema.oezyagan@partner.kit.edu (S. Özyagan).

https://doi.org/10.1016/j.apgeochem.2025.106465
Received 19 February 2025; Received in revised form 15 April 2025; Accepted 4 June 2025

2005) at low ionic strength (I_m(NaCl) = 0.03 mol kg^{-1}). Extrapolation to zero ionic strength yielded a $log\ K_m^0([CmH_3SiO_4]^{2+}) = 7.74 \pm 0.08$.

It is striking, that there is a lack of complexation data at elevated ionic strengths in chloride media. Such conditions are present in pore and formation waters of the clay rock formations in Northern Germany, which are considered as a potential site for a nuclear waste repository. Hence, the present work provides novel insights into the complexation of trivalent actinides with monosilicate at various ionic strength (I_m(NaCl) = 0.18 mol kg^{-1} to 3.00 mol kg^{-1}) at room and elevated temperatures. Cm(III) is used as a representative of the trivalent actinide ions due to its excellent spectroscopic properties which enables the study of the complexation reactions using time-resolved laser fluorescence spectroscopy (TRLFS).

2. Experimental section

2.1. Materials and instruments

2.1.1. TRLFS measurements

TRLFS measurements were performed using a Nd:YAG (Surelite II laser, Continuum) pumped dye laser system (NarrowScan D-R; Radiant Dyes Laser Accessories GmbH). Cm(III) was excited at a wavelength of 396.6 nm. A spectrograph (Shamrock 303i, ANDOR) with 300, 1199 and 2400 lines per millimeter gratings was used for spectral decomposition. The fluorescence emission was detected by an ICCD camera (iStar Gen III; ANDOR). All measurements were performed with a delay time of 1 μs to discriminate scattering light and short-lived organic fluorescence.

2.1.2. pH$_m$ titration

Sodium chloride (Merck, Purity >99 %) was of analytical grade and was used without further purification. An Orion Star (Fisher Scientific) pH meter and a micro glass combination electrode (Mettler Toledo) was used for the pH$_m$ measurements. Before measurement, the electrode was calibrated at pH$_m$ = 4.00 ± 0.01; 7.00 ± 0.01 and 10.01 ± 0.01 with NIST standard buffer solutions (Fisher Scientific). For all dilutions, MilliQ water was used. The silicic acid solutions were prepared by dilution of a silicon standard solution for ICP (1000 mg/L Si in 2 % NaOH, Merck) with 0.1 M HCl to Si concentrations below the solubility limit of amorphous silica (Lagerström, 1959), (Grenthe et al., 2020) ranging from 5•10^{-4} to 3.88•10^{-3} mol kg^{-1} (pH$_m$ ≈ 1.7). The TRLFS samples were prepared by adding 5.7 μL of a Cm(III) stock solution (2.12 • 10^{-5} M $Cm(ClO_4)_3$ in 0.1 M $HClO_4$; ^{248}Cm: 89.7 %, ^{246}Cm: 9.4 %, ^{243}Cm: 0.4 %, ^{244}Cm: 0.3 %, ^{245}Cm: 0.1 %, ^{247}Cm: 0.1 %) to 1200 μL of a silicic acid solution with I_m(NaCl) = 0.18 mol kg^{-1} to 3.00 mol kg^{-1}, resulting in a Cm(III) concentration of 10^{-7} mol kg^{-1}. All TRLFS samples were prepared in SUPRASIL-Quartz glass cuvettes (Hellma Analytics, 10 mm • 10 mm). The pH$_m$ of the solutions was varied from 4 to 6.5 with an interval of 0.1 for the spectroscopic speciation. For each ionic strength, the pH$_m$ of the solution was corrected according to the following equations (Eq. (1) and (2)) (Altmaier et al., 2003):

$$A_{NaCl} = -0.0988 + 0.1715 \cdot m_{NaCl} + 0.0013\,(m_{NaCl})^2 \tag{1}$$

$$pH_m = pH_{exp} + A_{NaCl} \tag{2}$$

2.1.3. Temperature dependent studies

The silicic acid solutions were prepared by dilution of a silicon standard solution for ICP (1000 mg^{-1} L Si in 2 % NaOH, Merck) with 0.1 M HCl to Si concentrations below the solubility limit of amorphous silica (Lagerström, 1959) ranging from 5•10^{-4} to 1.05•10^{-3} mol kg^{-1} (pH$_m$ = 1.7). For these studies, the ionic strength was varied from I_m(NaCl) = 0.01 mol kg^{-1} to 0.65 mol kg^{-1}. Note that A_{NaCl} in Eq. (2) is temperature dependent but was not corrected for higher temperatures as we assume that the temperature-induced changes are negligible in the studied ionic strength and temperature range. The pH$_m$ = 5.3 for T = 25 °C was adjusted and then the samples were heated to a temperature of T = 80 °C with intervals of 5–10 °C. Then, the sample was pre-equilibrated for 20 min and pH$_m$ of the sample was measured. The temperature was controlled by a thermostat.

3. Results and discussion

3.1. Complexation studies of $[Cm(H_3SiO_4)]^{2+}$ in chloride media

The chemistry of silicic acid is very complex (Dietzel, 2000), Panak et al. found the monosilicic complex species to only form in the pH$_m$ range of 4–7 and [Si] below 5•10^{-4} mol kg^{-1} (Panak et al., 2005). Accordingly, the complexation of Cm(III) with monosilicate in this work at various ionic strengths ranging from I_m(NaCl) = 0.18–3.00 mol kg^{-1} has also been studied in a pH$_m$ range between 4 and 6.5. Fig. 1 shows a selection of normalized emission spectra of Cm(III) with monosilicate as a function of the pH$_m$ for low (I_m(NaCl) = 0.01 mol kg^{-1}, left) and medium (I_m(NaCl) = 3.00 mol kg^{-1}, right) ionic strength. At low ionic strength and at pH$_m$ = 3.0, an emission band with a peak maximum at λ = 593.8 nm is observed. This band is assigned to the Cm^{3+} aquo ion (Beitz, 1991). With increasing pH$_m$, a bathochromic shift of the emission band is observed and a new emission band with a peak maximum at λ = 598.5 nm occurs. This resulting shoulder is more pronounced with increasing pH$_m$. This emission band has already been described as the $[Cm(H_3SiO_4)]^{2+}$ complex in the literature (Panak et al., 2005). At higher ionic strength, this bathochromic shift of the emission band is still visible, however it is very subtle. This trend is visible for all normalized Cm(III) emission spectra of $[Cm(H_3SiO_4)]^{2+}$ as a function of pH$_m$ at various ionic strengths, see Fig. S1 in the Supporting Information (SI).

The complexation is described by the following complexation model:

$$Cm^{3+} + H_3SiO_4^- \rightleftharpoons [Cm(H_3SiO_4)]^{2+} \tag{3}$$

The conditional stability constant is calculated according to the law of mass action:

$$K_m = \frac{[Cm(H_3SiO_4)\,]^{2+}}{[Cm^{3+}]\cdot[H_3SiO_4]^-_{free}} \tag{4}$$

Slope analyses were performed according to Eq. (5):

$$\log\left(\frac{[Cm(H_3SiO_4)\,]^{2+}}{[Cm^{3+}]}\right) = \log K_m + \log\,[H_3SiO_4]^-_{free} \tag{5}$$

The free silicate concentration, $[H_3SiO_4]^-_{free}$ is given by Eq. (6):

$$[H_3SiO_4]^-_{free} = [H_3SiO_4]^- - [Cm^{3+}]\cdot\chi_{1:1} \tag{6}$$

$X_{1:1}$ represents the molar fraction of the Cm(III) silicate complex species. $[H_3SiO_4]^-$ is obtained from the total silicic acid concentration by considering the pK_a value of silicic acid and the pH$_m$ value of the sample solution (c. f. Eq. (7)). The pK_a value is given in the literature: $pK_a = 9.82$ at zero ionic strength (Busey and Mesmer, 1977). However, the pK_a value changes with increasing ionic strength (c.f. Table S1 in the SI), which was also considered in the complexation model.

$$[H_3SiO_4]^- = [H_4SiO_4]\cdot 10^{(pHm-pKa)} \tag{7}$$

$X_{1:1}$ is obtained from the emission spectra by peak deconvolution. The single component spectra used for this iterative process as well as an example of peak deconvolution are given in Fig. S2 and S3 in the SI. Slope analyses are performed according to Eq. (3), for which log $[H_3SiO_4]^-_{free}$ was plotted against log $\left(\frac{[Cm(H_3SiO_4)]^{2+}}{[Cm^{3+}]}\right)$. The linear regression yields a slope of 0.99 ± 0.01 and confirms the 1:1 stoichiometry of $[Cm(H_3SiO_4)]^{2+}$ (c.f. Fig. 2, red) for I_m(NaCl) = 0.01 mol kg^{-1}. Accordingly, for I_m(NaCl) = 3.00 mol kg^{-1}, a slope of 1.04 ± 0.04 was obtained (c.f. Fig. 2, black). For all slope analyses at various ionic strengths, see Fig. S4 in the SI. Comparing the concentration ratios in Fig. 2 for low and increased ionic strength, it is evident that a higher concentration of free

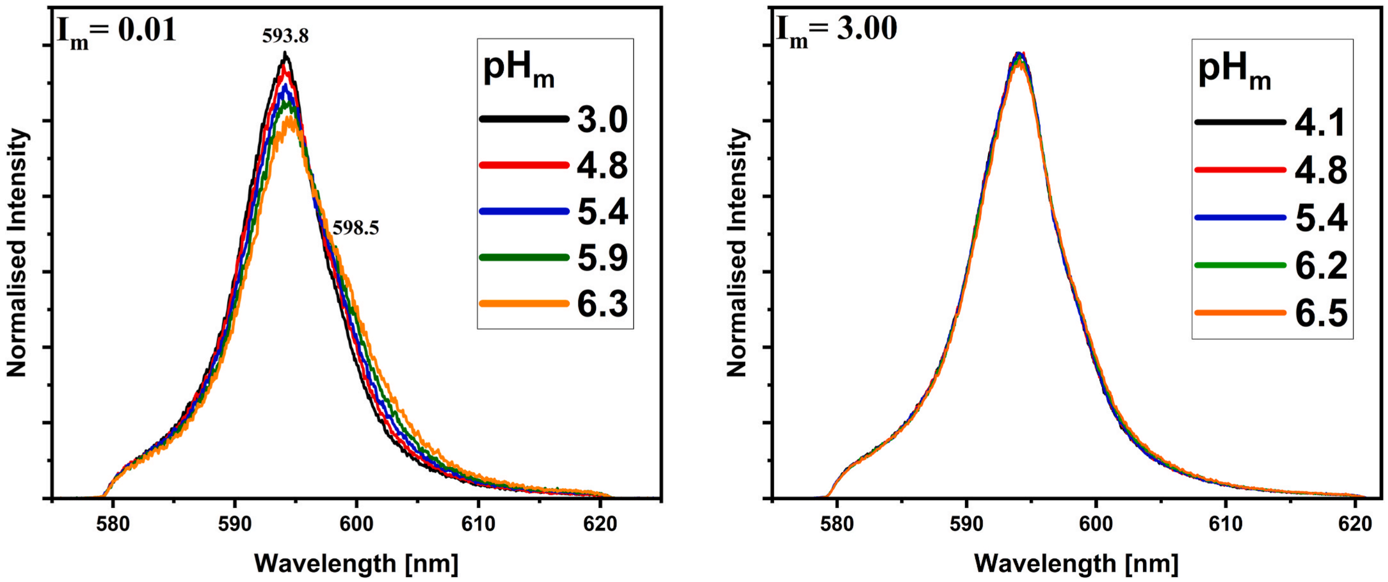

Fig. 1. Normalized Cm(III) emission spectra with a Si concentration [Si] = 1.05 10^{-3} mol kg^{-1} as a function of pH_m, [Cm] = 10^{-7} mol kg^{-1}, I_m = 0.01 mol kg^{-1} (left) and I_m = 3.00 mol kg^{-1}(right), T = 25 °C.

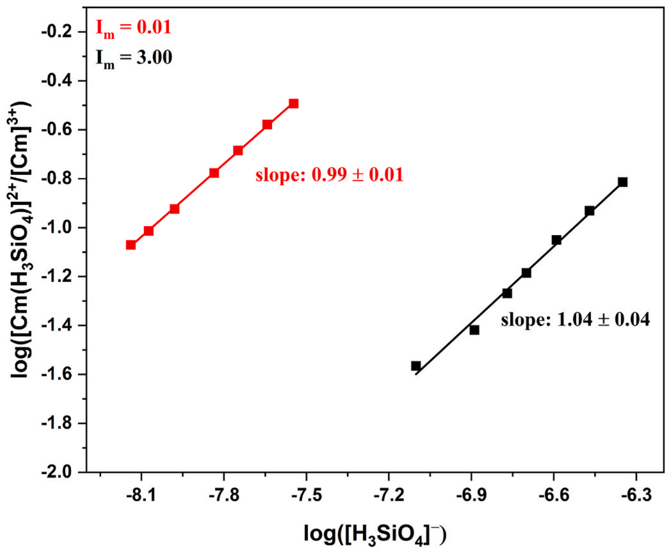

Fig. 2. Slope analyses for the complexation of Cm(III) with monosilicate for I_m(NaCl) = 0.01 mol kg^{-1} (red) and I_m(NaCl) = 3.00 mol kg^{-1} (black), T = 25 °C. Plot of log ($[Cm(H_3SiO_4)]^{2+}/[Cm^{3+}]$) versus the logarithm of $[H_3SiO_4]^-_{free}$. (For interpretation of the references to colour in this figure legend, the reader is referred to the Web version of this article.)

Table 1
Conditional stability constants of the complexation of Cm(III) with monosilicate as a function of ionic strength, T = 25 °C.

I_m [mol kg^{-1}]	$\log K_m$
0.18	7.2 ± 0.7
0.35	7.2 ± 0.7
0.65	6.9 ± 0.7
1.18	6.5 ± 0.7
2.23	6.3 ± 0.6
2.57	6.0 ± 0.6
3.00	5.9 ± 0.6

silicates are required to form $[Cm(H_3SiO_4)]^{2+}$. The conditional stability constants of the complexation of Cm(III) with monosilicate as a function of ionic strength are given in Table 1.

As shown in Table 1, for the investigated chloride system as background electrolyte ranging from I_m (NaCl) = 0.18–3.00 mol kg^{-1}, we observe a decline from $\log K_m\left([Cm(H_3SiO_4)]^{2+}\right) = 7.2 \pm 0.7$ to $\log K_m\left([Cm(H_3SiO_4)]^{2+}\right) = 5.9 \pm 0.6$. This indicates that the increase in ionic strength leads to a decrease of the complex stability of $[Cm(H_3SiO_4)]^{2+}$ by 1.3 orders of magnitude.

Thakur et al. determined $\log K_m\left([Cm(H_3SiO_4)]^{2+}\right) = 7.78 \pm 0.02$ for the Cm-monosilicate $[Cm(H_3SiO_4)]^{2+}$ and $\log K_m\left([Eu(H_3SiO_4)]^{2+}\right) = 7.81 \pm 0.01$ for the Eu-monosilicate $[Eu(H_3SiO_4)]^{2+}$ at I_m ($NaClO_4$) = 0.20 mol kg^{-1} using solvent extraction (pH_m = 3.50, [Si] = 2•10^{-3} – 2•10^{-2} mol kg^{-1}) (Thakur et al., 2007). Comparing our data to these conditional stability constants of $[M(H_3SiO_4)]^{2+}$ with M = Cm, Eu in the perchlorate system, it is evident that with $\log K_m\left([Cm(H_3SiO_4)]^{2+}\right) = 7.2 \pm 0.7$ at I_m (NaCl) = 0.18 mol kg^{-1}, the formation of $[Cm(H_3SiO_4)]^{2+}$ in the chloride system is less favored by approximately 0.6 orders of a magnitude. This is in line with the slightly higher complexation strength of chloride in comparison to perchlorate. Thakur et al. also performed studies on the formation of Cm-monosilicate at higher ionic strengths in the $NaClO_4$ system. It was found that the conditional stability constant of $[Cm(H_3SiO_4)]^{2+}$ decreases from $\log K_m\left([Cm(H_3SiO_4)]^{2+}\right) = 7.78 \pm 0.08$ at I_m ($NaClO_4$) = 0.20 mol kg^{-1} to $\log K_m\left([Cm(H_3SiO_4)]^{2+}\right) = 7.37 \pm 0.13$ at I_m ($NaClO_4$) = 1.00 mol kg^{-1} (Thakur et al., 2007). This trend is in excellent agreement with the results observed for the chloride system in our work.

3.2. *Specific ion interaction theory*

For better comparison with literature data and implementation into thermodynamic data bases, $\log K_m^0$ at zero ionic strength is determined. Unlike the conditional stability constants $\log K_m$ at varying ionic strengths, the $\log K_m^0$ at zero ionic strength cannot be determined experimentally. For extrapolation to zero ionic strength, the SIT is used. The SIT model describes the activity coefficients of species *i* in aqueous solution according to the following equation (Guggenheim, 1935)' (Guggenheim and Turgeon, 1955):

$$\log \gamma_i = -z_i^2 \frac{A(T)\sqrt{I_m}}{1+B(T)a_i\sqrt{I_m}} + \sum \varepsilon(i,k)\,(T)\cdot m_k \tag{8}$$

Here, z_i is the charge of ion i, $\varepsilon\,(i,k)$ is the ion interaction coefficient of opposite charged ions i and k, m_k

(mol kg^{-1}) is the molal concentration of ion k and $\frac{A(T)\sqrt{I_m}}{1+B(T)a_i\sqrt{I_m}}$ is the temperature dependent Debye-Hückel term D(T). A(T) and B(T) are Debye-Hückel parameters. a_i is an ion size parameter for the hydrated ion i, while I_m is the molal ionic strength. $A(T)$ and $B(T)a_i$ as a function of temperature are listed in the NEA-TDB (Grenthe et al., 2020). The stability constant $\log K_m^0$ and $\Delta\varepsilon$ at zero ionic strength is derived from the conditional stability constants $\log K_m$ at $I_m(NaCl) = 0.18$ mol kg^{-1} to 3.00 mol kg^{-1} by linear regression according to Eq. (9):

$$\log K_m - \Delta z^2 \cdot D = \log K_m^0 - \Delta\varepsilon \cdot I_m \tag{9}$$

$$\Delta\varepsilon = \sum \varepsilon_{products} - \sum \varepsilon_{educts} \tag{10}$$

Therefore, $\log K_m - \Delta z^2 \cdot D$ is plotted against the ionic strength I_m. The linear SIT regression plot at T = 25 °C is depicted in Fig. 3. The intercept with the y-axis corresponds to $\log K_m^0$ at zero ionic strength. However, $\Delta\varepsilon$ is determined from the slope. From the linear SIT regression plot, $\log K_m^0\left([Cm(H_3SiO_4)]^{2+}\right) = 8.1 \pm 0.8$ and $\Delta\varepsilon = 0.25 \pm 0.01$ kg mol^{-1} are obtained. To determine the binary ion-ion interaction coefficient $\varepsilon([Cm(H_3SiO_4)]^{2+}, Cl^-)$, the following interaction coefficients are used as given in the NEA-TDB (Lemire et al., 2013): $\varepsilon(Am^{3+}, Cl^-) = 0.23 \pm 0.02$ kg mol^{-1} (as a substitute for the unknown $\varepsilon(Cm^{3+}, Cl^-)$) and $\varepsilon(Na^+, H_3SiO_4^-) = -0.08 \pm 0.03$ kg mol^{-1}. The binary ion-ion interaction coefficient for the Cm-monosilicate complex is calculated according to the following equation:

$$\varepsilon\left([Cm(H_3SiO_4)]^{2+}, Cl^-\right) = \Delta\varepsilon + \varepsilon\left(Na^+, H_3SiO_4^-\right) + \varepsilon\left(Am^{3+}, Cl^-\right) = 0.40 \pm 0.04 \text{ kg mol}^{-1} \tag{11}$$

Table 2 shows the $\log K_m^0\left([Cm(H_3SiO_4)]^{2+}\right)$ for the formation of $[Cm(H_3SiO_4)]^{2+}$ of the present work and other stability constants at zero ionic strength, which have been determined in the literature. Panak et al. studied the formation of $[Cm(H_3SiO_4]^{2+}$ in chloride medium at only one single ionic strength ($I_m(NaCl) = 0.03$ mol kg^{-1}) by TRLFS. The $\log K_m^0\left([Cm(H_3SiO_4)]^{2+}\right)$ was determined via a single point extrapolation. Thakur et al. determined $\log K_m^0\left([Cm(H_3SiO_4)]^{2+}\right)$ in perchlorate media ($I_m(NaClO_4) = 0.20$ mol kg^{-1} to 1.00 mol kg^{-1}) by solvent extraction. Both literature values show deviations from the $\log K_m^0\left([Cm(H_3SiO_4)]^{2+}\right)$ value of our work. Nevertheless, in this present study, the formation of $[Cm(H_3SiO_4)]^{2+}$ was studied systematically in an ionic strength range up to 3.00 mol kg^{-1}. Through these systematic investigations at a wide ionic strength range, the stability constant $\log K_m^0\left([Cm(H_3SiO_4)]^{2+}\right) = 8.1 \pm 0.8$ is based on a broader data set compared to other literature studies. In addition, the $\log K_m^0\left([M(H_3SiO_4)]^{2+}\right)$ value in the NEA-TDB, which is an averaged stability constant for the formation of $[M(H_3SiO_4)]^{2+}$ (with M = Eu(III), Cm(III) and Am(III)) is in excellent agreement with the value determined in our work.

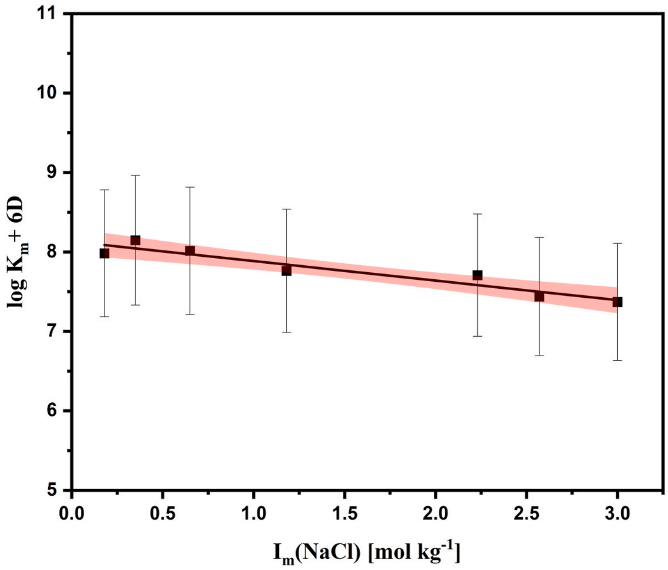

Fig. 3. Plot of $\log K_m$+ 6D vs. the ionic strength I_m and fitting according to the SIT equation at T = 25 °C for the complexation reaction: $Cm^{3+} + H_3SiO_4^- \rightarrow [Cm(H_3SiO_4)]^{2+}$.

Table 2
Comparison of $\log K_m^0$ (this work) with literature data for $[M(H_3SiO_4)]^{2+}$ (M = Cm, Eu, Am) at T = 25 °C.

	Method	$\log K_m^0$	Reference
$[Cm(H_3SiO_4)]^{2+}$	TRLFS	8.1 ± 0.8	p. w.
$[Cm(H_3SiO_4)]^{2+}$	TRLFS	7.74 ± 0.08	Panak et al. (Panak et al., 2005)
$[Cm(H_3SiO_4)]^{2+}$	Extraction	8.60 ± 0.08	Thakur et al. (Thakur et al., 2007)
$[M(H_3SiO_4)]^{2+}$ (M = Cm, Eu, Am)	Extraction	8.13 ± 0.20	NEA-TDB[a] (Grenthe et al., 2020)

[a] Averaged stability constant for the formation of $[M(H_3SiO_4)]^{2+}$ (M = Eu(III), Cm(III) and Am(III)) listed in the NEA-TDB.

3.3. Determination of thermodynamic data for the formation of $[Cm(H_3SiO_4)]^{2+}$ in chloride media

To determine thermodynamic data ($\Delta_r H_m$; $\Delta_r S_m$) of the complex formation of $[Cm(H_3SiO_4)]^{2+}$, studies at elevated temperatures were conducted. For those studies, the ionic strength range and Si concentrations were carefully selected to reduce the risk of the formation of Cm-polysilicates ($[Si] < 5{\bullet}10^{-3}$ mol kg^{-1} (Busey and Mesmer, 1977) and $I_m < 1$ mol kg^{-1} (Kitahara, 1960)). For lower ionic strengths $I_m < 0.65$ mol kg^{-1}, a Si concentration of $[Si] = 5{\bullet}10^{-4}$ mol kg^{-1}, at higher ionic strengths ($I_m \geq 0.65$ mol kg^{-1}) a Si concentration of $1.05{\bullet}10^{-3}$ M was used. The slightly higher Si concentration was required to compensate for the increasing repression of $[Cm(H_3SiO_4)]^{2+}$ at higher ionic strength. The pH_m was adjusted to 5.3. The temperature was varied between 10 and 80 °C. In Fig. 4, the normalized Cm(III) emission spectra as a function of temperature are depicted. With increasing temperature, the emission band shifts to higher wavelengths and a hot band appears at 585 nm (Lindqvist-Reis et al., 2005). The intensity of the band at 593.8 nm (Cm aquo ion) decreases, while the intensity of the band at 598.5 nm ($[Cm(H_3SiO_4)]^{2+}$) increases at rising temperatures. From this observation, it is evident that the formation of $[Cm(H_3SiO_4)]^{2+}$ is an endothermic reaction. After evaluation of the emission spectra by peak deconvolution, $\log K_m(T)$ were determined for each ionic strength. At $I_m(NaCl) = 0.01$ mol kg^{-1}, $\log K_m\left([Cm(H_3SiO_4)]^{2+}, T\right)$ is 7.2 ± 0.7 at T = 10 °C and increases to 7.7 ± 0.8 at T = 75 °C, while at $I_m(NaCl) = 0.65$ mol kg^{-1}, $\log K_m\left([Cm(H_3SiO_4)]^{2+}, T\right)$ is 6.6 ± 0.7 at T = 10 °C and increases to 7.2 ± 0.7 at T = 75 °C. In both cases, there is an increase in the conditional stability constants of about half an order of magnitude with increasing temperatures. The temperature dependent conditional stability constants at each ionic strength are used for the determination of the reaction enthalpy $\Delta_r H_m$ and the reaction entropy $\Delta_r S_m$ according to the Van't Hoff equation (c.f. Eq. (10)). Applying this equation, it is assumed that the heat capacity of the reaction equals zero in the

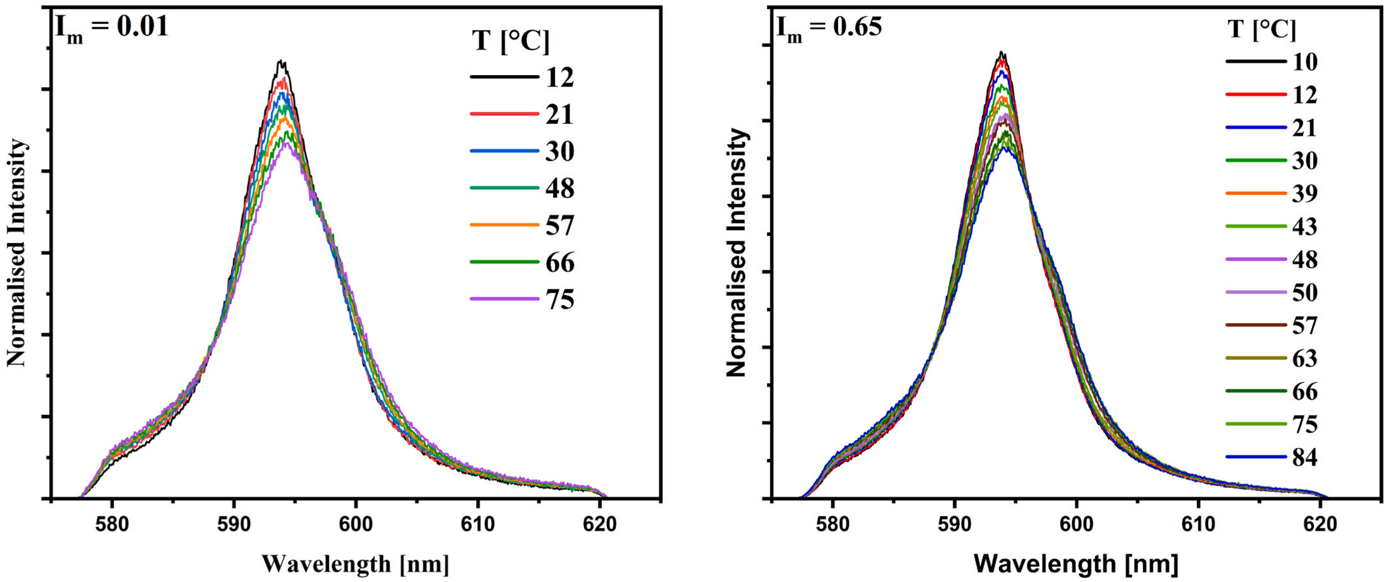

Fig. 4. Normalized Cm(III) emission spectra as a function of temperature with a Si concentration [Si] = 5•10^{-4} mol kg^{-1}, [Cm] = 10^{-7} mol kg^{-1}, I_m = 0.01 mol kg^{-1} (left) and with a Si concentration [Si] = 1.05•10^{-3} mol kg^{-1}, [Cm] = 10^{-7} mol kg^{-1}, I_m = 0.65 mol kg^{-1} (right).

temperature range studied ($\Delta_r C_{p,m} = 0$) (Atkins and Paula, 2010) and thus, the standard molar reaction enthalpy is constant:

$$\log\ K_m(T) = \frac{1}{2.3R}\cdot\left(\Delta_r S_m - \frac{\Delta_r H_m}{T}\right) \qquad (12)$$

In Fig. 5, the determined $\log K_m\left([\mathrm{Cm(H_3SiO_4)}]^{2+}, \mathrm{T}\right)$ are plotted as a function of the reciprocal temperature. For the low ionic strength, $\Delta_r H_m = 15.3$ kJ K^{-1} mol^{-1} and $\Delta_r S_m = 191.5$ J K^{-1} mol^{-1}, for the higher ionic strength $\Delta_r H_m = 9.6$ kJ mol^{-1} and $\Delta_r S_m = 164.7$ J $K^{-1}mol^{-1}$ were determined. These results confirm that the complexation reaction is endothermic and entropy driven in the ionic strength range studied. Nevertheless, with an increase in ionic strength, the reaction enthalpy $\Delta_r H_m$ and reaction entropy $\Delta_r S_m$ decreases (see Table 3). This means that the temperature dependence of the complexation reaction is reduced at higher ionic strength and the increase in the temperature dependent conditional stability constant is less pronounced. For all temperature dependent studies at various ionic strengths, see Fig. S5 in the SI.

Table 3
Reaction entropies and enthalpies for the formation of $[\mathrm{Cm(H_3SiO_4)}]^{2+}$ at various ionic strengths.

I_m [mol kg^{-1}]	$\Delta_r H_m$ [kJ mol^{-1}]	$\Delta_r S_m$ [J $K^{-1}mol^{-1}$]
0.01	15.3	191.5
0.35	12.4	180.0
0.50	10.5	167.4
0.65	9.6	164.7

3.4. Extrapolation of the reaction enthalpy to zero ionic strength

By the use of an enthalpy specific SIT plot, the ionic strength dependent reaction enthalpies are extrapolated to zero ionic strength (see Fig. 6). The standard reaction enthalpy is determined according to Eq. (11) (Skerencak-Frech et al., 2019).

$$\Delta_r H_m - \Delta z^2 \cdot D_L = \Delta_r H_m^0 - RT^2 \Delta\varepsilon_L \cdot I_m \qquad (13)$$

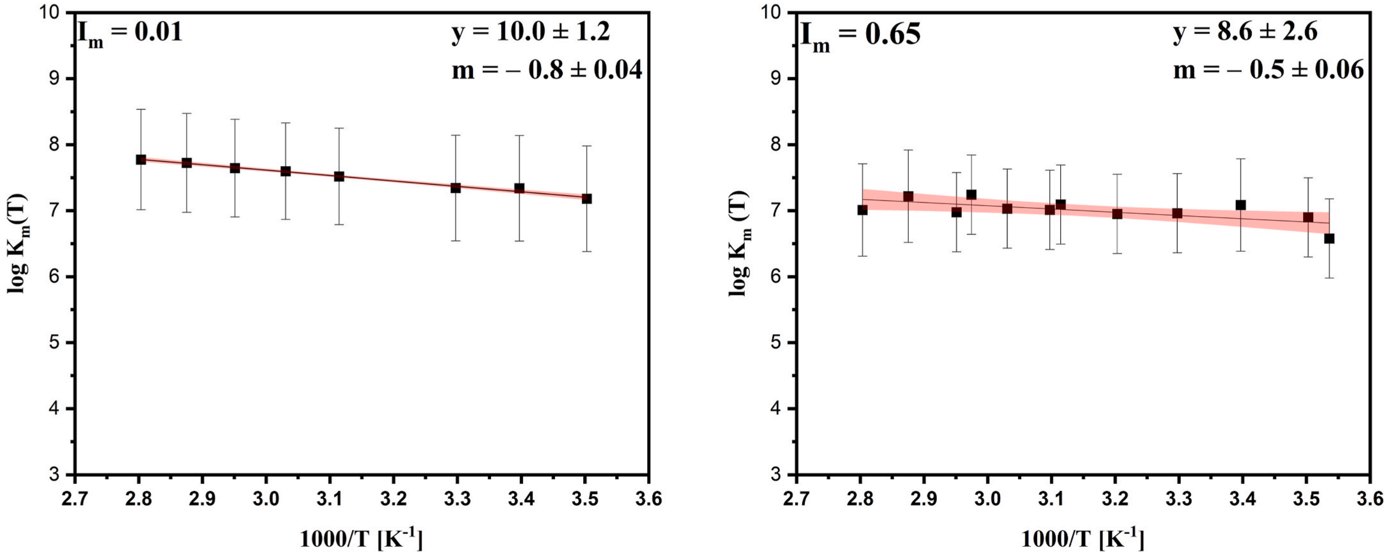

Fig. 5. Plot of $\log K_m(T)$ vs T^{-1} and fitting according to the van't Hoff equation for I_m(NaCl) = 0.01 mol kg^{-1} (left), I_m(NaCl) = 0.65 mol kg^{-1} (right) at T ≈ 10–80 °C.

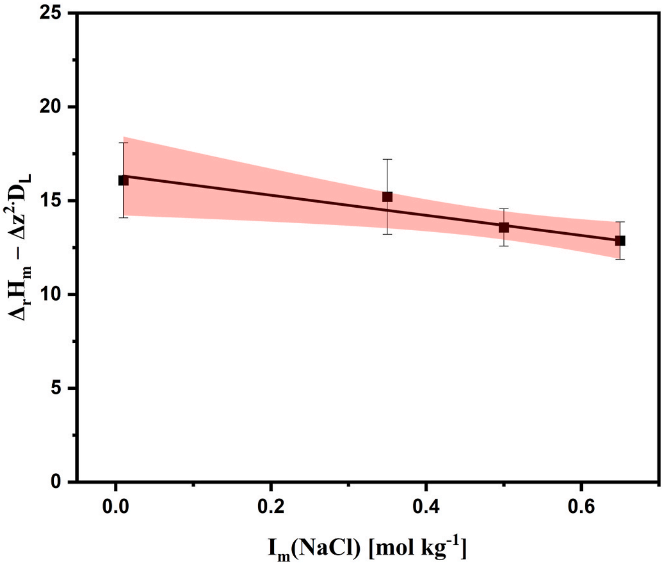

Fig. 6. Plot of $\Delta_r H_m$ -$\Delta z^2 \cdot D_L$ vs. the ionic strength I_m and fitting according to the enthalpy specific SIT equation for I_m(NaCl) = 0.01 up to 0.65 mol kg^{-1}.

With $D_L = \frac{0.75 \cdot 1.989 \cdot \sqrt{I_m}}{1+1.5\sqrt{I_m}}$ and $\Delta\ \varepsilon_L\ = \sum_i \varepsilon_L\ (i,k)$, with the latter being the relative partial molar enthalpy specific ion interaction coefficient.

Applying the Van't Hoff equation, the standard reaction enthalpy $\Delta_r H^0_m$ = 16.4 ± 0.5 kJ mol^{-1}, the standard reaction entropy $\Delta_r S^0_m$ = 210 ± 21 J K^{-1} mol^{-1} and the free Gibbs energy $\Delta_r G^0_m$ = - 46.2 ± 5 kJ mol^{-1} were determined. At standard state conditions, the complexation reaction is endothermic and entropy driven. Only one study on thermodynamic data for $[Cm(H_3SiO_4)]^{2+}$ is available in the literature. Pathak et al. determined the standard reaction enthalpy $\Delta_r H^0_m$ = 18.6 ± 4.0 kJ mol^{-1} for $[Cm(H_3SiO_4)]^{2+}$ and $\Delta_r H^0_m$ = 17.3 ± 1.0 kJ mol^{-1} for $[Eu(H_3SiO_4)]^{2+}$ by solvent extraction (Grenthe et al., 2020). These literature values however were determined in a very limited temperature range (T = 5–45 °C) through extrapolation of a single point calculation ($I_m(NaClO_4)$ = 0.20 mol kg^{-1}). In comparison to the literature, the enthalpy specific SIT plot in our work is based on various ionic strengths (I_m(NaCl) = 0.01 – 0.65 mol kg^{-1}) and a broader temperature range up to T = 80 °C. However, the literature values are in excellent agreement with the $\Delta_r H^0_m$ in our work.

4. Conclusions

The complexation of Cm(III) with monosilicate was investigated by TRLFS in 0.18–3.00 mol kg^{-1} NaCl solutions. The results show that the formation of the monosilicate complex $[Cm(H_3SiO_4)]^{2+}$ is decreased with increasing ionic strength, leading to a decrease of the conditional stability constants of 1.3 orders of a magnitude. Using the specific ion interaction theory, the complexation constant at zero ionic strength $\log K^0_m\left([\mathrm{Cm(H_3SiO_4)}]^{2+}\right) = 8.1 \pm 0.8$ and the binary ion-ion interaction coefficient ε ($[Cm(H_3SiO_4)]^{2+}$,Cl^-) = 0.40 ± 0.04 kg mol^{-1} were determined. Additionally, the formation of $[Cm(H_3SiO_4)]^{2+}$ was studied at temperatures ranging from 10 to 80 °C at various ionic strengths. With an enthalpy specific SIT plot, thermodynamic data at standard state conditions were determined ($\Delta_r H^0_m$ = 16.4 ± 0.5 kJ mol^{-1}, $\Delta_r S^0_m$ = 210 ± 21 J K^{-1} mol^{-1} and $\Delta_r G^0_m$ = – 46.2 ± 5.0 kJ mol^{-1}). These results confirm that the formation of $[Cm(H_3SiO_4)]^{2+}$ is an endothermic entropy driven complexation reaction.

Cementitious materials are a part of the multi-barrier system considered for nuclear waste repositories. Through natural water intrusion over time, a release of increased amounts of Si might occur. The clay formations located in Northern Germany contain pore and formation waters with ionic strengths up to 3 mol kg^{-1}. They are considered as a potential site for a nuclear waste repository. Consequently, it is of utmost importance to study the complexation of actinides with silicates in aqueous systems as a function of ionic strength. With this work, a first step of understanding the influence of medium ionic strength on complex reactions at standard state conditions is accomplished. The present results provide a complexation constant and thermodynamic data for implementation into thermodynamic data bases, taking us one step further in grasping the complexation behavior of very complex An(III) silicate systems under various near-field conditions of different nuclear waste repositories.

CRediT authorship contribution statement

Sema Özyagan: Writing – review & editing, Writing – original draft, Formal analysis, Data curation. **Kim J. Warth:** Investigation, Formal analysis, Data curation. **Thomas Sittel:** Writing – review & editing, Validation, Supervision. **Petra J. Panak:** Writing – review & editing, Validation, Supervision, Project administration, Funding acquisition.

Associated content

Supporting Information available: TRLFS spectra: SIT plot, Van't Hoff plots.

Declaration of competing interest

The authors declare that they have no known competing financial interests or personal relationships that could have appeared to influence the work reported in this paper.

Acknowledgements

This work was supported by the Federal Ministry for Environment, Nature Conservation, Nuclear Safety and Consumer Protection (BMUV) under contract number 02E11860H.

Appendix A. Supplementary data

Supplementary data to this article can be found online at https://doi.org/10.1016/j.apgeochem.2025.106465.

Data availability

Data will be made available on request.

References

Altmaier, M., Metz, V., Neck, V., Müller, R., Fanghänel, T., 2003. Geochem. Cosmochim. Acta 67, 3595–3601.
Atkins, P., Paula, J.d., 2010. Physical Chemistry, ninth ed. W. H. Freeman Co, New York.
Beitz, J.V., 1991. Radiochim. Acta 52–53, 35–40.
Busey, R.H., Mesmer, R.E., 1977. Inorg. Chem. 16, 2444–2450.
G. R. Choppin, P. Pathak, P. Thakur, 2008, 31, 53-72.
Coradin, T., Eglin, D., Livage, J., 2004. Spectroscopy 18, 356207.
Dietzel, M., 2000. Geochem. Cosmochim. Acta 64, 3275–3281.
Grenthe, I., Plyasunov, A.V., Runde, W.H., Konings, R.J.M., Moore, E.E., Gaona, X., Rao, L., Grambow, B., Smith, A.L., 2020. (OECD, NEA-TDB): Vol. 14. Second Update on the Chemical Thermodynamics of Uranium, Neptunium, Plutonium, Americium and Technetium, OECD Nuclear Energy Agency Data Bank. OECD Publishing, Paris, France.
Guggenheim, E., 1935. Lond. Edinb. Dubl .Phil. Mag 19, 588–643.
Guggenheim, E.A., Turgeon, J.C., 1955. Trans. Faraday Soc. 51, 747–761.
Jensenf, M.P., Choppin, G.R., 1996. Radiochim. Acta 72, 143–150.
Kim, M.A., Panak, P., Yun, J.-I., Kim, J.I., Klenze, R., Köhler, K., 2003. Colloids Surf., A: Physicochem. Eng. 216, 97–108.
Kim, J.-I., 2008. In: Kim, Y.J., Platt, U. (Eds.), Advanced Environmental Monitoring. Springer Netherlands, Dordrecht, pp. 233–247.
Kitahara, S., 1960. Rev. Phys. Chem. Jpn. 30.
Lagerström, G., 1959. Acta Chem. Scand. 13, 722–736.

Lemire, R.J., Berner, U., Palmer, D.A., Musikas, C., Tochiyama, O., Taylor, P., 2013. (OECD, NEA-TDB). Chemical Thermodynamics of Iron, Part 1. OECD Nuclear Energy Agency Data Bank, vol. 13a. OECD Publishing, Paris, France.

Lindqvist-Reis, P., Klenze, R., Schubert, G., Fanghänel, T., 2005. J. Phys. Chem. B 109, 3077–3083.

Moll, H., Geipel, G., Brendler, V., Bernhard, G., Nitsche, H., 1998. J. Alloys Compd. 271–273, 765–768.

P. J. Panak, M. A. Kim, R. Klenze, J.-I. Kim, T. Fanghänel, 2005, 93, 133-139.

Pathak, P.N., Choppin, G.R., 2006. Radiochim. Acta 94, 81–86.

Porter, R.A., Weber, W.J., 1971. J. Inorg. Nucl. Chem. 33, 2443–2449.

Ray, N.H., Plaisted, R.J., 1983. J. Chem. Soc. Dalton Trans. 475–481.

Satoh, I., Choppin, G.R., 1992. Radiochim. Acta 56, 85–88.

Skerencak-Frech, A., Taube, F., Zanonato, P.L., Acker, M., Panak, P.J., Di Bernardo, P., 2019. Thermochim. Acta 679, 178316.

Thakur, P., Singh, D.K., Choppin, G.R., 2007. Inorg. Chim. Acta. 360, 3705–3711.

Titulaer, M.K., Kegel, W.K., Jansen, J.B.H., Geus, J.W., 1994. J. Non-Cryst. Solids 170, 128–133.

Wadsak, W., Hrnecek, E., Irlweck, K., 2000. Radiochim. Acta 88, 61–64.